

BSC contribution to INDECIS D6.2

Jaume Ramon and Llorenç Lledo
Barcelona Supercomputing Center

Summary

An intercomparison of two global widely used reanalysis datasets with reference data has been performed in terms of wind speeds, Capacity Factor (CF) and Wind Power Density (WPD). Both CF and WPD are energy indices extensively used within the wind energy field to anticipate the power production or evaluate the performance of a running wind farm, among others. The three parameters are computed using the ERA5 and MERRA2 reanalyses at 77 locations where high-quality data is available from instrumented tall towers. A comparison with these data reveals that the reanalyses generally underestimate seasonal mean wind speeds, and thus CF and WPD are underestimated as well. However, the ERA5 shows better correlations than MERRA2 for all three studied parameters. We recommend using the ERA5 near surface wind fields to estimate monthly wind speeds and CFs, whereas the ERA5 surface winds appear to be a better source to derive accurate estimates of WPD.

Wind energy indices: Capacity Factor and Wind Power Density

The Capacity Factor (CF) is an index used within the wind power sector to assess the performance or usage of any generating power plant, no matter their sizes. For a given period, it is calculated dividing the produced generation by the maximum production that would be achieved if the plant were operating at full capacity during all the time:

$$CF = \frac{\text{produced power} \in \text{atimeperiod}t}{\text{maximum produced power} \in \text{atimeperiod}t}$$

Usually expressed as a percentage, it may also be interpreted as the proportion of time that the plant would have to be working at full capacity to produce the same amount of energy produced. The conversion between wind speed and power output is usually made employing power curves, which are provided by the turbine manufacturers and take into account the specific efficiency characteristics of the turbine model. Then, the capacity factor can be derived from power curve values easily, dividing power output by the nominal capacity of the turbine.

The international standard IEC-61400-1 (IEC, 2005) defines four classes of wind turbines (type I, II, III and IV) depending on the mean and peak wind speeds in the area where the wind farm is planned to be installed. Type I turbines are suited for areas with high annual average wind speeds (10 ms^{-1}), so they are physically heavy to withstand heavy loads. Taking this classification into account, the CF can also be defined to each one of the turbine classes (CF1, CF2, CF3, and

CF4).

CF also gives an idea of how good are the atmospheric conditions for producing energy during a specific period in a wind farm.

Wind Power Density (WPD) is another wind energy index that does not depend on technological factors. The meteorological factors upon which wind power generation depends are wind speed (v) and air density (ρ). Particularly, the kinetic energy of the wind blowing through a square metre of air (also referred to as Wind Power Density, WPD) is:

$$WPD = \frac{1}{2} \rho v^3, \text{ where } \rho = \frac{p}{R_d T} \text{ (} R_d = 287.05 \text{ J/kg)}$$

Therefore WPD indicates the total kinetic energy that is available in the wind for extraction and conversion to electricity. The efficiency in converting to electricity depends on the employed technology and can vary a lot (Burton et al., 2001).

Data and methods

The ECVs that have been assessed are surface (10-metre) and near-surface (50 and 100 metres) wind speeds from the ERA5 (Copernicus Climate Change Service, 2017) and MERRA2 (Molod et al., 2015) reanalyses. These reanalysis wind fields will be verified against in situ quality-controlled data taken at several tall tower locations and collected within the Tall Tower Dataset (Ramon and Lledó, 2019). These high vertical structures measure wind speeds at many heights above ground, usually ranging from 10 to 200 metres above ground level. In our work, we have selected as observational reference the tower measuring level which is closest to 100 metres. To provide robust verification results, we have carefully selected those towers containing time series spanning at least three years. A total of 77 series from locations distributed worldwide (see Figure 1) have been employed.

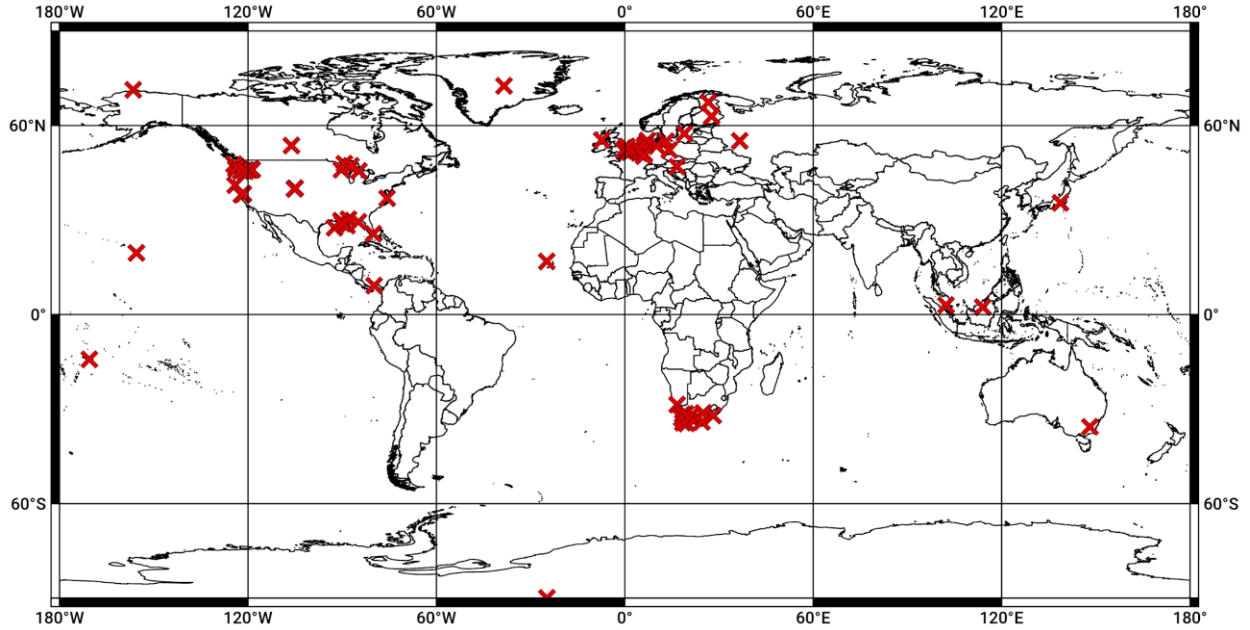


Figure 1.- Global distribution of the 77 tall towers.

In addition to the wind speeds, the two relevant indices for the wind power industry, CF and WPD, have been computed from reanalyses and tower locations and evaluated as well. In the case of CF, turbine classes I, II and III will be considered, and a CF for each turbine class will be examined. For that purpose, three manufacturer-provided power curves have been used (Lledó et al., 2019).

Reanalysis data are first interpolated horizontally by taking the closest grid point to the tower location. The intercomparison of wind speed and WPD is performed at the selected tower measuring heights. To vertically extrapolate reanalysis surface and near surface winds (WS) to the tower measuring heights (h), a power law equation has been assumed:

$$WS(h) = WS(h_{ref}) \left(\frac{h}{h_{ref}} \right)^\alpha \quad \alpha = 0.143 \text{ for inland sites; } \alpha = 0.11 \text{ for water bodies}$$

Where h_{ref} is the reference height of the reanalysis field (i.e., 10, 50 or 100 metres). The comparison of the CF, however, is done at 100 metres, since the power curves are explicitly meant for 100-meter height wind turbines. We note that in this case, tall tower winds also need to be extrapolated vertically to 100 metres.

Monthly averages of wind speeds and the two indices are first compared in terms of correlation, standard deviation, and centered root mean squared error (CRMSE). A Taylor diagram (Taylor, 2001) is employed here to visualise those three parameters in one single graph. Then, seasonal averages are prepared and compared among them.

Results

Surface and near surface wind speeds

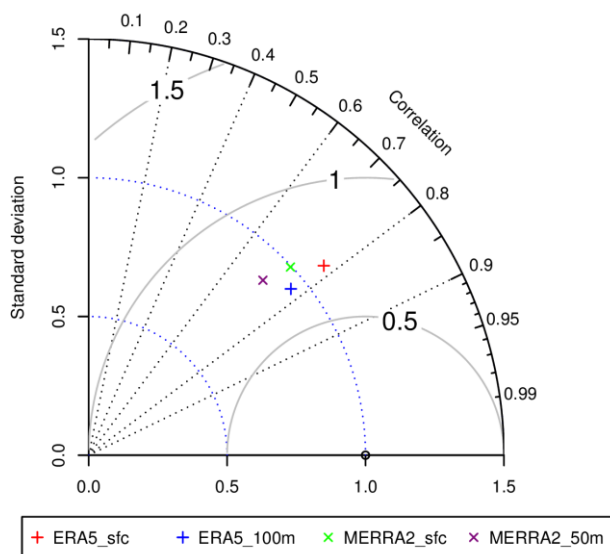


Figure 2.- Taylor diagram of the pairwise observed and reanalysis monthly-averaged winds. Radial dimension represents the model standard deviations normalised by the observations'. Pearson correlation coefficients are represented in the angular coordinate whereas the arcs show the CRMSEs.

Monthly-averaged wind speeds from both reanalysis and tall towers are compared by means of a Taylor diagram in Figure 2. We note that in general, the ERA5 provides better correlations and lower CRMSEs than MERRA2. The comparison with the observed variability, however, reveals that the near surface winds offer less variability than surface winds from both reanalysis datasets. These differences in variability between surface and near-surface wind fields are mainly produced by the power law extrapolation, which effects are more appreciable in the extrapolation of the surface wind fields. Overall, the ERA5 near-surface winds offer the closest results to the observed.

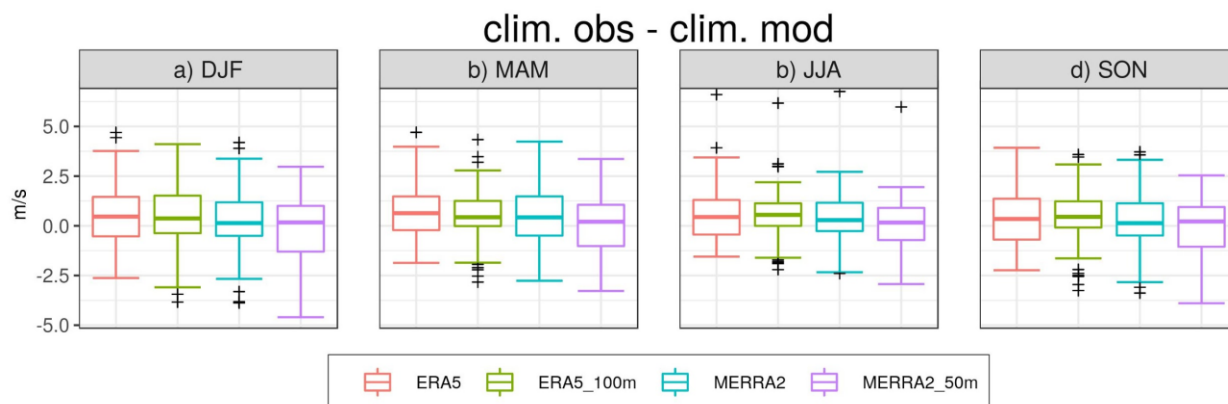


Figure 3.- Boxplots summarising the differences between observed (*obs*) and reanalysis (*mod*) seasonal

climatologies for 77 tall towers in (a) December-January-February, (b) March-April-May, (c) June-July-August and (d) September-October-November.

Seasonal averages of wind speeds have also been prepared and intercompared. The distribution of the differences between observed and reanalysis seasonal averages at the 77 tall tower sites is presented in box plots in Figure 3. The range of the differences is rather similar for the four datasets. Overall, an underestimation of the seasonal averages by the reanalyses is observed. The widest dispersion is observed in DJF (Figure 3a). The wide range of differences observed is probably related to the representativeness errors of reanalyses gridded products, i.e. its inability to represent the spatial variability within a grid cell.

Capacity factor

Taylor diagrams presenting the intercomparison of the CFs for the turbine types I, II and III computed using the surface and near surface winds from ERA5 and MERRA2 are shown in Figure 4. Once again, ERA5 presents better correlations and lower CMRSEs than MERRA2. In terms of variability, it is observed that the vertical extrapolation of the ERA5 surface winds derives in an excess of variability in all three CFs. However, the ERA5 near surface winds, which are already delivered at the 100-metre level, match the observed variability of the three CFs at the tower locations. Also, MERRA2 surface winds reproduce well the observed variability but show lower correlations than ERA5.

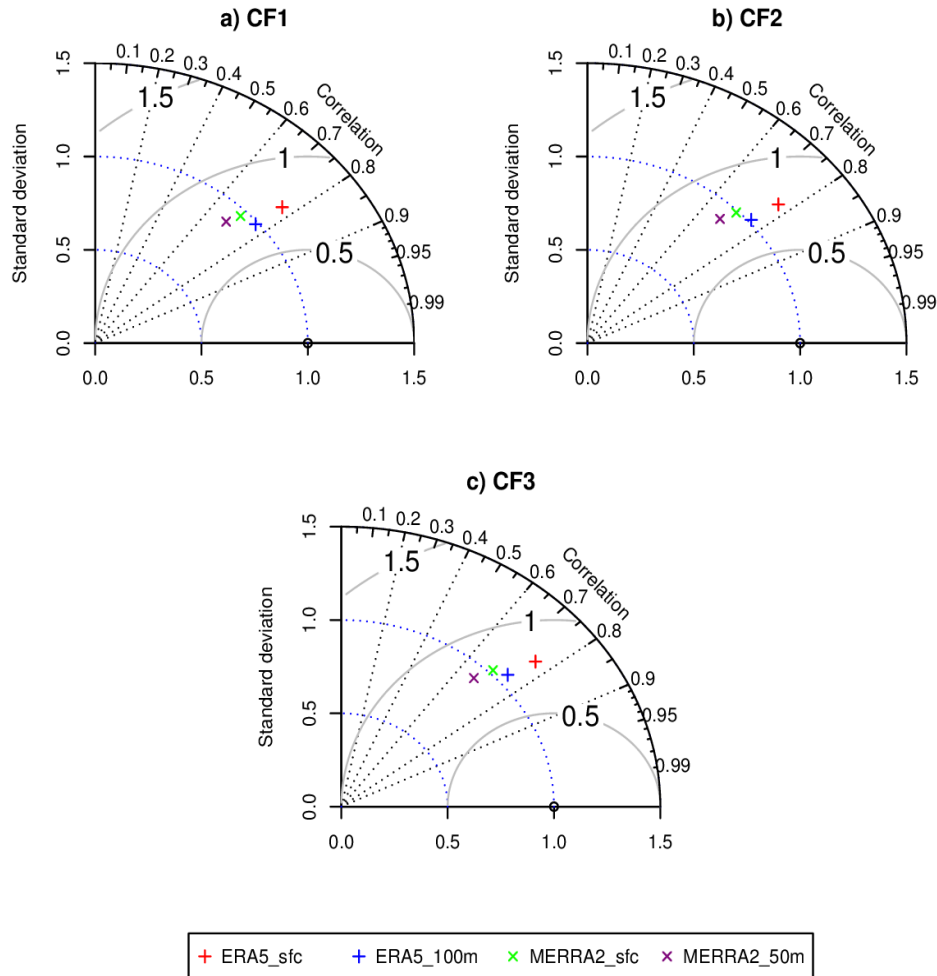


Figure 4.- Taylor diagram of the pairwise monthly observed and reanalysis-derived (a) CF1, (b) CF2 and (c) CF3. Radial dimension represents the model standard deviations normalised by the observations'. Pearson correlation coefficients are represented in the angular coordinate whereas the arcs show the CRMSEs.

Seasonal averages of CF1, CF2 and CF3 are also compared at the tall tower locations, and the differences between those computed with the set of reanalysis datasets are plotted in Figures 5, 6 and 7. Similarly to Figure 3, none of the reanalysis stands out in any of the target seasons. However, we notice that the median of the differences for the MERRA2 near surface winds is very close to zero in all the CFs (Figures 5, 6 and 7). Despite this, the range of the differences is as wide as the observed for the other datasets, so it cannot be concluded that NASA's reanalysis outperforms the ERA5 wind fields. Concerning also the width of the distribution of the differences, we note that CF3 shows the widest range of values reaching up to 0.5.

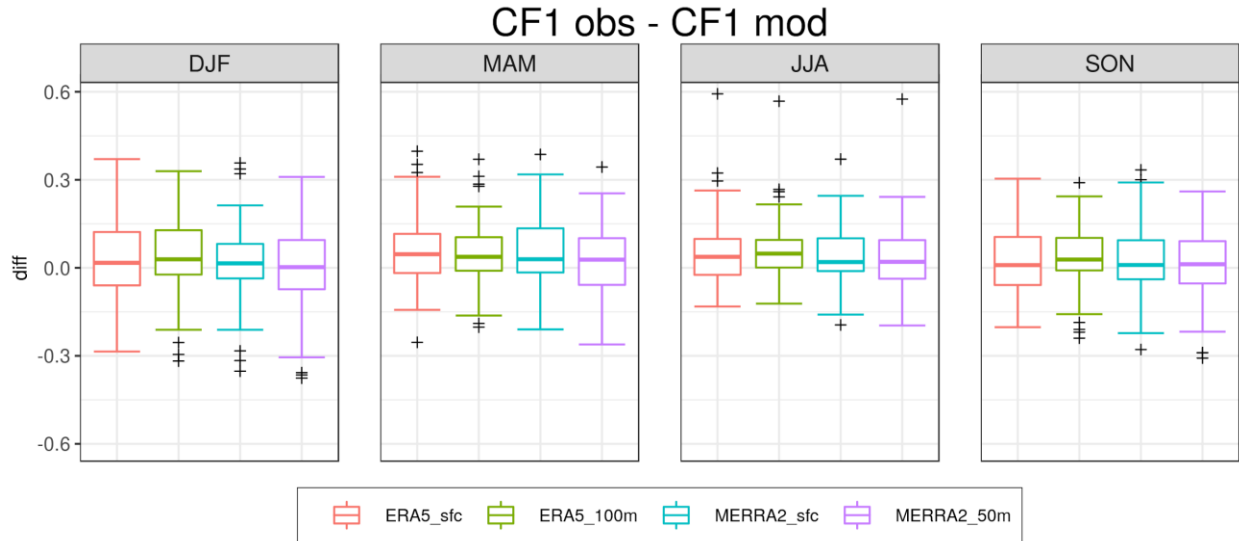


Figure 5.- Boxplots summarising the differences between observed (*obs*) and reanalysis (*mod*) CF1 seasonally aggregated for 77 tall towers in (a) December-January-February, (b) March-April-May, (c) June-July-August and (d) September-October-November.

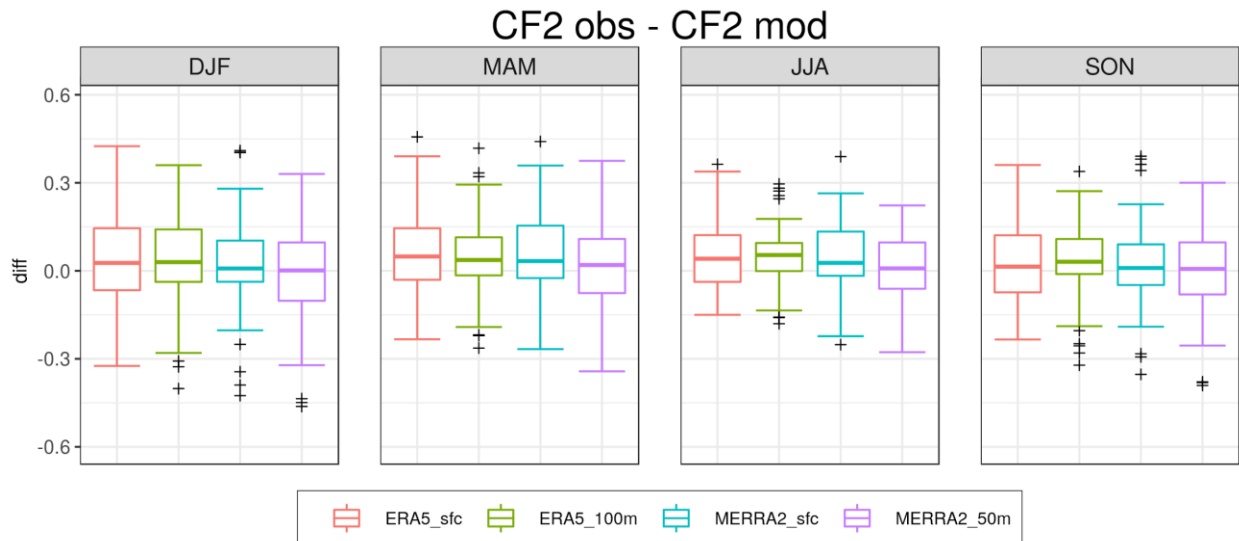


Figure 6.- Boxplots summarising the differences between observed (*obs*) and reanalysis (*mod*) CF2 seasonally aggregated for 77 tall towers in (a) December-January-February, (b) March-April-May, (c) June-July-August and (d) September-October-November.

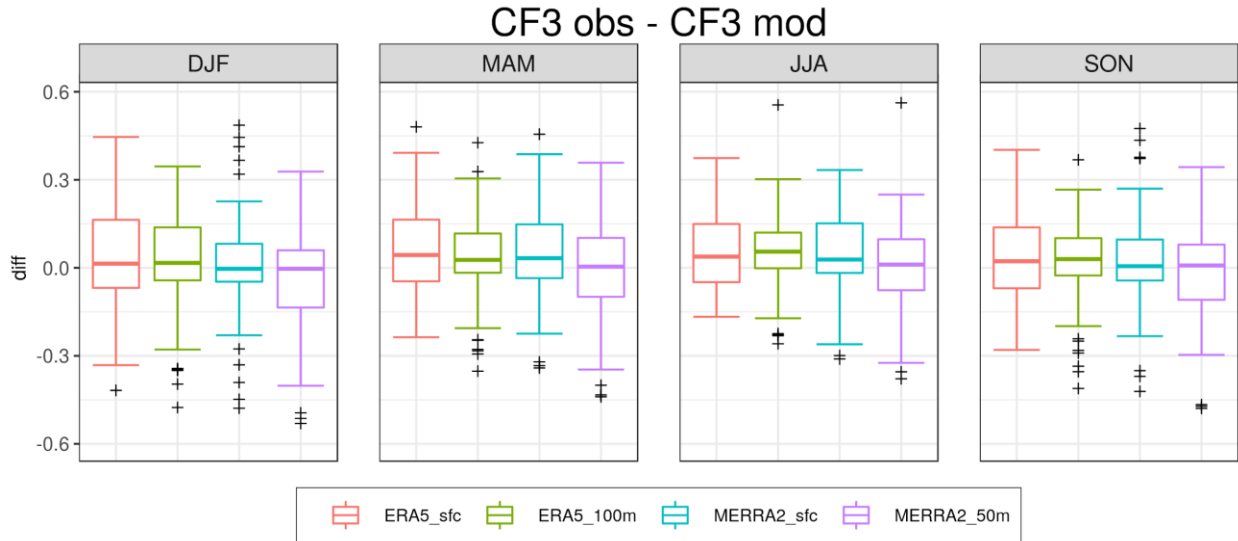


Figure 7.- Boxplots summarising the differences between observed (*obs*) and reanalysis (*mod*) CF3 seasonally aggregated for 77 tall towers in (a) December-January-February, (b) March-April-May, (c) June-July-August and (d) September-October-November.

Wind Power Density

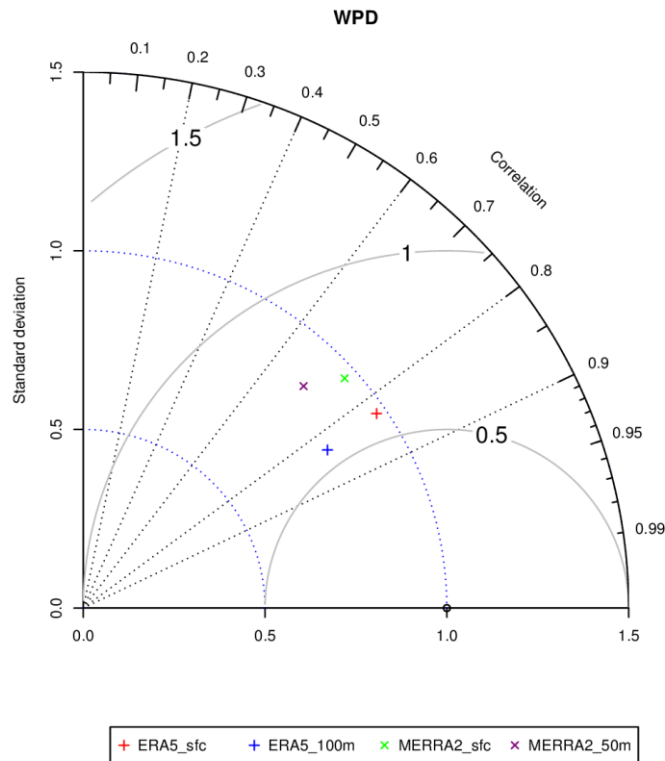


Figure 8.- Taylor diagram of the pairwise monthly observed and reanalysis-derived WPDs. Each point corresponds to one specific tall tower and reanalysis. Radial dimension represents the model standard deviations normalised by the observations'. Pearson correlation coefficients are represented in the angular coordinate whereas the arcs show the CRMSEs.

Figure 8 presents the Taylor diagram for the comparison of the WPD computed from the tall towers and the observations. In general, reanalyses correlate better with WPD than CF. The variability, however, differs substantially from the observed, being underestimated in all cases. Even though the 100-metre wind dataset correlates slightly better with the observed WPDs, the estimates from the ERA5 surface winds offer the closest results to reality.

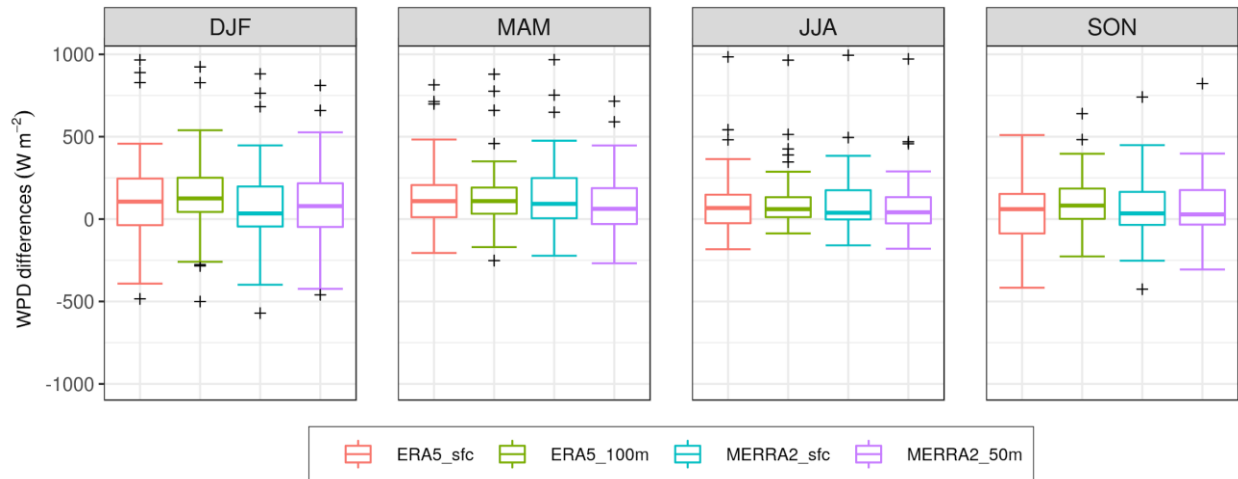


Figure 9.- Boxplots summarising the differences between observed (*obs*) and reanalysis (*mod*) WPD seasonally aggregated for 77 tall towers in (a) December-January-February, (b) March-April-May, (c) June-July-August and (d) September-October-November.

Seasonal averages of WPD are also intercompared by means of box plots in Figure 9. As in Figure 8, seasonal averages of WPD are also underestimated by the reanalyses. The widest dispersion of differences between observed and modelled WPD is noticed in DJF (Figure 9(a)), whereas the narrowest range of values is noticed in JJA (Figure 9(c)). Concerning the reanalyses, ERA5 winds show the narrowest boxes, even though the WPD estimates appear systematically biased in all seasons. This bias is less appreciable in MERRA2, but the range of differences is larger for this reanalysis.

Conclusions

Global reanalysis datasets are needed in seasonal forecasting for many purposes such as bias correction of these predictions as well as their verification. Currently, only the ERA5 and MERRA2 global reanalysis offer 1-hourly data at relatively fine resolution (0.3° and 0.5°x0.625°, respectively). Nevertheless, some remarks should be made concerning their representation of wind speeds, CF and WPD.

Reanalyses hardly reproduce the monthly-averaged wind speeds, and these biases are also observed after deriving the CF and WPD indices. Since global reanalyses are provided in a coarse

grid (31 km of resolution as maximum), they are unable to reproduce local features such as local winds or turbulence that may occur at a much finer spatial scales within the grid cell. Nonetheless, many wind energy applications can benefit from the reanalysis data, specially at 1-hourly time scale.

ERA5 provides better correlations and lower CRMSEs than MERRA2 for the three analysed variables. The ERA5 near-surface winds appear like a good approach to derive monthly averaged winds and CFs, whereas the ERA5 surface winds offer the best results to compute the WPD. Finally, it is also worth noting that the surface wind field datasets, when extrapolated to either tower measuring level or the 100-metre height, show systematically higher variability than the extrapolation of the near surface winds to the same level. We argued that this excess of variability is introduced by the power law approach used in the vertical extrapolation of winds.

References

- Burton, T., D. Sharpe, N. Jenkins, and E. Bossanyi, 2001: Wind Energy Handbook. John Wiley & Sons, Ltd, 617 pp.
- Copernicus Climate Change Service (C3S), 2017: ERA5: Fifth generation of ECMWF atmospheric reanalyses of the global climate. Copernicus Climate Change Service Climate Data Store (CDS).
- IEC, International Standard IEC 61400-1, third ed., 2005
- Lledó, L., V. Torralba, A. Soret, J. Ramon, and F. J. Doblas-Reyes, 2019: Seasonal forecasts of wind power generation. *Renew. Energy*, 143, 91–100, <https://doi.org/10.1016/j.renene.2019.04.135>.
<https://linkinghub.elsevier.com/retrieve/pii/S0960148119306196>.
- Molod, A., L. Takacs, M. Suarez, and J. Bacmeister, 2015: Development of the GEOS-5 atmospheric general circulation model: Evolution from MERRA to MERRA2. *Geosci. Model Dev.*, 8, 1339–1356, <https://doi.org/10.5194/gmd-8-1339-2015>.
- Ramon, J., and LI. Lledó, 2019: The Tall Tower Dataset. Technical Note. 45 pp. https://earth.bsc.es/wiki/lib/exe/fetch.php?media=library:external:technical_memoranda:technical_report_talltower_database_v2.pdf.